PHOTOGRAPH THIS SHEET

AD A095063

DTIC ACCESSION NUMBER

LEVEL

INVENTORY

AEC

Rpt. No. WT-356

DOCUMENT IDENTIFICATION

June 1952

DISTRIBUTION STATEMENT A

Approved for public release;
Distribution Unlimited

DISTRIBUTION STATEMENT

ACCESSION FOR		
NTIS	GRA&I	☒
DTIC	TAB	☐
UNANNOUNCED		☐
JUSTIFICATION		
BY (June 1952)		
DISTRIBUTION /		
AVAILABILITY CODES		
DIST	AVAIL AND/OR SPECIAL	
A		

Released

DISTRIBUTION STAMP

DTIC
ELECTE
JAN 6 1981
S D
D

DATE ACCESSIONED

UNANNOUNCED

DATE RECEIVED IN DTIC

PHOTOGRAPH THIS SHEET AND RETURN TO DTIC-DDA-2

DTIC FORM OCT 79 70A

DOCUMENT PROCESSING SHEET

UNCLASSIFIED

[redacted]

TECHNICAL LIBRARY
AUG 12 1957
of the
ARMED FORCES
SPECIAL WEAPONS PROJECT
20777

WT-356

Copy No. 287 A

27993

Operation

BUSTER - JANGLE

NEVADA PROVING GROUNDS
OCTOBER - NOVEMBER 195

Project 10.6

THE MEASUREMENT OF GAMMA-RAY INTENSITY VS TIME

RESTRICTED DATA

This document contains restricted data as defined in the Atomic Energy Act of 1946. Its transmittal or the disclosure of its contents in any manner to an unauthorized person is prohibited.

CANCELLED

AD A995063

Classification (Cancelled) [redacted] to
By Authority of Ex Rev. DNA/DOE
By K. Ali, Jr. CL ISC m Date 30 Jul 82

Classification
By Authority of

80 12 15 10

LOS ALAMOS SCIENTIFIC LABORATORY
UNIVERSITY OF CALIFORNIA

Statement A
Approved for public release;
Distribution unlimited.

UNCLASSIFIED

[redacted]

SECRET
SECURITY INFORMATION

WT-356

UNCLASSIFIED

This document consists of 37 pages
No. 287 of 300 copies, Series A

THE MEASUREMENT OF GAMMA-RAY INTENSITY VS TIME

Operation Buster-Jangle

by

JOHN S. MALIK

RESTRICTED DATA
This document contains restricted data as defined in the Atomic Energy Act of 1946. Its transmittal or the disclosure of its contents in any manner to an unauthorized person is prohibited.

Los Alamos Scientific Laboratory
Los Alamos, New Mexico

June 1952

UNCLASSIFIED

SECRET
SECURITY INFORMATION

UNCLASSIFIED

ABSTRACT

Gamma-ray intensity vs time data in the range from a few milliseconds to about 20 sec were obtained on tests C and E of Operation Buster and the underground test (Shot F) of Operation Jangle. The equipment consisted of a detector consisting of a solution of terphenyl in toluene surrounding a coaxial phototube, the output of which was fed into a 5.5-decade pseudo-log circuit which in turn was direct-coupled to the plates of a 3-in. battery-operated scope tube. The face of the scope was photographed with a 16-mm strip-film camera.

The data seem to indicate that the source of the gamma radiation for these times is due to neutron capture in the nitrogen of the air, followed in about 0.2 sec by gamma rays from the decay of fission fragments, the latter modified by shock hydrodynamics and rise of the fireball.

[redacted]

UNCLASSIFIED

ACKNOWLEDGMENTS

Assistance in the performance of this experiment is gratefully acknowledged to the following: R. Patten, R. Feynman, and others of LASL Group P-1 who supplied and helped calibrate the detectors used in the experiment; to N. H. Smith and H. K. Stephenson, who formed the "labor pool" for the placement and removal of sandbags before and after the tests; and to R. H. Campbell, who designed the recording cans.

[redacted]

CONTENTS

		Page
ABSTRACT		5
ACKNOWLEDGMENTS		7
1	INTRODUCTION	11
2	EQUIPMENT	12
3	CALIBRATION	18
4	RESULTS	18
APPENDIX A	PSEUDO-LOG CIRCUIT	31
APPENDIX B	SHIELDING MEASUREMENTS	33

ILLUSTRATIONS

1	P-2 $\gamma(t)$ Data	13
2	View of Detector	14
3	Buster Pseudo-log Circuit	15
4	Pseudo-log Circuit Characteristic	16
5	Timing Oscillator	17
6	Control Circuit	17
7	Recording Unit Removed from Can	19
8	Station 961 and Equipment	20
9	Recording Unit in Culvert	21
10	Station 961 Ready for a Shot	22
11	Gamma Intensity vs Time, Buster C	24
12	Integral of Curve of Fig. 11	25
13	Gamma Intensity vs Time, Buster E	26
14	Integral of Curve of Fig. 13	27
15	Gamma Intensity vs Time, Jangle F	28
A.1	Pseudo-log Circuit Characteristics for Various Values of Alpha	32

TABLES

1	Summary of Data	23
B.1	Shielding Measurements, Baker Test	33
B.2	Shielding Measurements, Dog Test	34

[redacted]

THE MEASUREMENT OF GAMMA-RAY INTENSITY VS TIME

1. INTRODUCTION

In order to understand properly the gamma radiation from a nuclear explosion and how the total dose is affected by changing design and firing conditions, it is necessary to know something about the source, its strength and location as a function of time, and also the behavior of the shocked air between the source and the point in question. As a start on the problem, knowledge of the intensity vs time of the gamma rays at one or two points is desired in order to make some guesses as to the source and how it is modified by the shock wave. The experiments conducted at this time were intended to obtain data which would be suitable for this purpose.

At the end of Operation Greenhouse some such data did exist as the result of experiments performed by the National Bureau of Standards group under L. Taylor and H. O. Wyckoff, and as the result of independent experiments carried out on the Item test by B. Watt and J. Malik. The data obtained by the Bureau were sparse and open to question. Those obtained by Watt and Malik agreed quite well, but there were differences in intensities which were outside the expected error of the measurements. These could be blamed on the equipment which was assembled in the field or possibly upon the differences in the location, since the detectors were at different heights and cable shielding mounds could have made the difference. Both these experiments had time resolutions on the order of 1 msec, and recording time was some 20 sec.

The picture which seemed to fit the data was that for times from a few milliseconds to about ¼ sec the gamma rays were due to neutron capture in the nitrogen of the air. For times longer than this the activity seemed to be due entirely to fission fragments and was strongly affected by the shock wave, which altered the amount of material between the fission-fragment source and the detector.

The mean life of a neutron in air of standard density, assuming a 1/v cross section with a value for thermal neutrons of 1.85 barns,[1] is 59 msec. For Nevada conditions the computed mean life is about 73 msec and for Eniwetok about 66 msec. The air density in the neighborhood of an explosion is not constant but can attain a maximum density of six times normal at the shock front if a constant gamma is assumed. The average density prior to shock arrival is, however, the original density. A rather rough calculation, based on an analytical expression for the density variation behind the shock wave and assuming that the source of gamma radiation is essentially at the shock front, indicates that the measured gamma-ray intensity should still fall at a rate about equal to the capture rate of the neutrons, at least for small bombs. For a gadget of 100 kilotons the effect is roughly to increase the apparent mean life about 10 per cent. (For a few-megaton gadget, however, the effect of the shock may be such as to lose the exponential fall and to produce a rise in intensity in this region.) During this period the source is probably a shell source essentially at the shock front, since both most of the air and most of the neutrons are in that region.

[redacted]

After the neutron-capture level has dropped to relatively low values, the decay of fission fragments becomes the predominant gamma-ray source. The decay rate, as measured in the laboratory, shows no short-lived periods, the shortest half life being about 0.43 sec followed by one of 1.5 sec,[2] the intensity falling like $t^{-1.2}$ in a few seconds. An expression[3] for the gamma-ray source strength of fission fragments from a slug of U^{235} after activation by neutrons from the water boiler is

$$7.6 \times 10^{-12}\ e^{-0.106 \ln^2 10.5t} \text{ curies per fission}$$

(see Fig. 1). The calibration is in terms of a radium source using a brass-walled roentgen chamber.

2. EQUIPMENT

The detector used in all these measurements was the same type as that used in the measurement of alpha. It consists of an RCA C-7154 coaxial phototube surrounded by a 5-cm-thick solution of terphenyl in toluene. This assembly was shock-mounted inside a cast aluminum dome for blast protection, the lower end of the active volume being at ground level (see Fig. 2). The phototube had a cylindrical photocathode of nickel coated with S-4 phosphor surrounded by the anode made of nickel mesh. The cathode had a diameter of 3.9 cm and an active length of 20 cm. The diameter of the anode was 8.13 cm and that of the glass envelope was 10 cm. This tube was mounted in an aluminum can of 20 cm diameter with a polyethylene seal between the can and phototube. The reasons for selecting such a detector were that it had about the proper sensitivity for use with the electronic equipment contemplated; it was constructed of low-atomic-number materials so that the output was approximately proportional to roentgens; calibration facilities existed; and, above all, the assembly was readily available. Further, most short-time data on gamma rays to date have been obtained by the use of such a detector, and for reasons of data comparison it was convenient to continue using it.

The detector was connected via a short coaxial line to a pseudo-log circuit of a 5.5-decade dynamic range using two steps per decade (Fig. 3). This circuit consists of a series of biased diodes connected so that, as the current input to the circuit increases, the load resistor in series with the phototube decreases in logarithmic steps. The resistors are so chosen that another diode is automatically switched in when the current increases by $10^{1/2}$. This gives a current input vs voltage output characteristic which is nearly linear between switching levels, with the switching levels lying on a straight line when the characteristic is plotted as the logarithm of current vs voltage. The deviation from true log response for the case of steps of $10^{1/2}$ is 8 per cent, but since this deviation is known this may be removed by an appropriate correction. The computed characteristic is shown in Fig. 4.

The output of this pseudo-log circuit was direct-coupled to the plates of a battery-operated 3-in. cathode-ray tube, the face of which was photographed along with a neon timing light with a 16-mm Cine Kodak E camera modified for continuous motion photography. The film speed used was about 3 ft/sec, the record being taken on 100-ft rolls of Linagraph Pan film. The timing neon light was driven by a Wien-bridge oscillator (Fig. 5), the output of which was squared up and then differentiated before being fed to the neon bulb.

The equipment was entirely battery operated, requiring only timing signals (-5 min for turning on filaments and -5 sec for starting the camera motor). The control circuit used is shown in Fig. 6.

The stations used for the experiment were designed to provide good shielding from gamma rays and neutrons with moderate cost and to permit easy recovery of the records. They consisted of a detector mount of concrete near an 18-in. culvert-lined hole 16 ft deep, the top 3-ft portion of the hole being enlarged to 4 ft in diameter to permit placing of the control relays, the log circuit, and batteries for filaments and camera under some sandbag shielding. The camera, the scope and its battery supply, and the timing oscillator were all mounted inside an aluminum

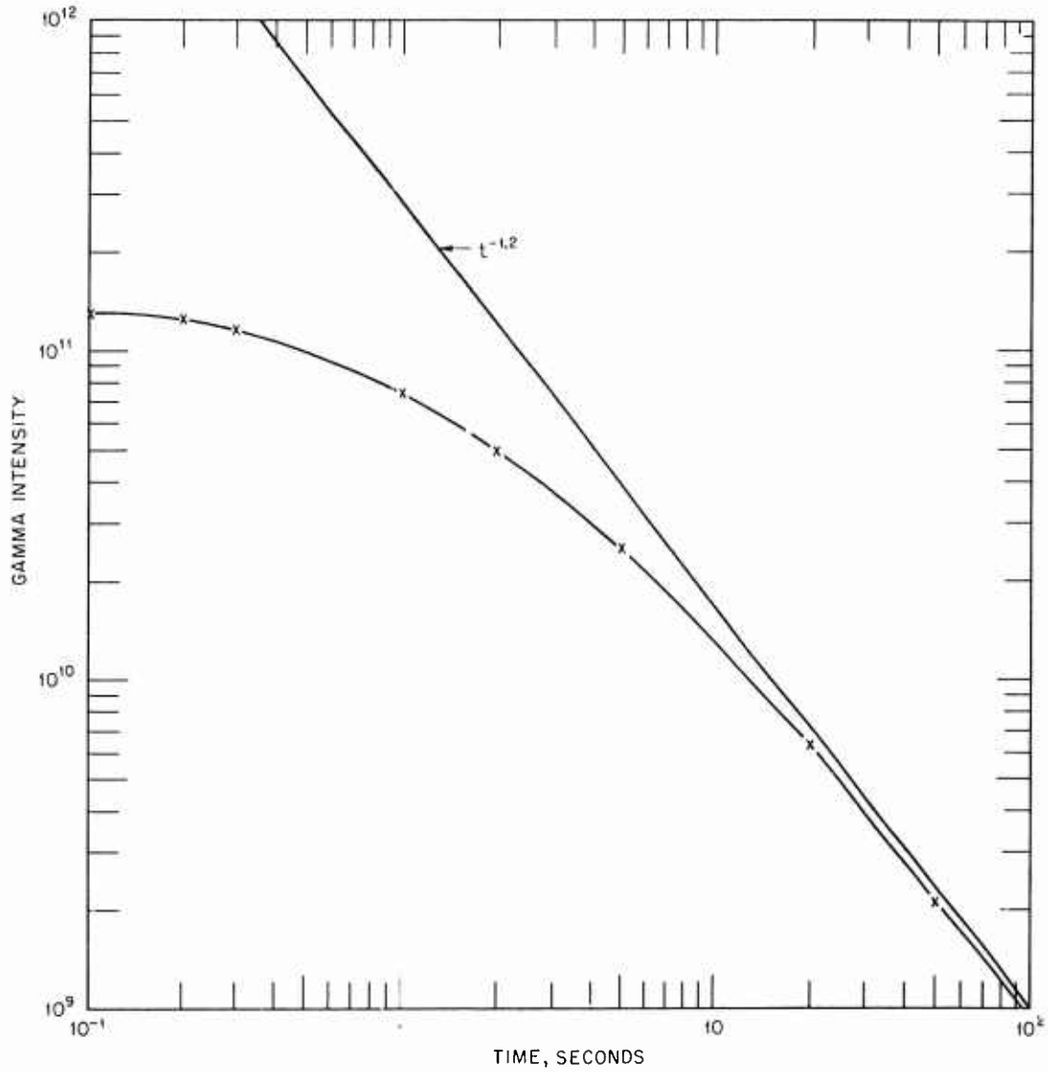

Fig. 1 — P-2 $\gamma(t)$ data.

[redacted]

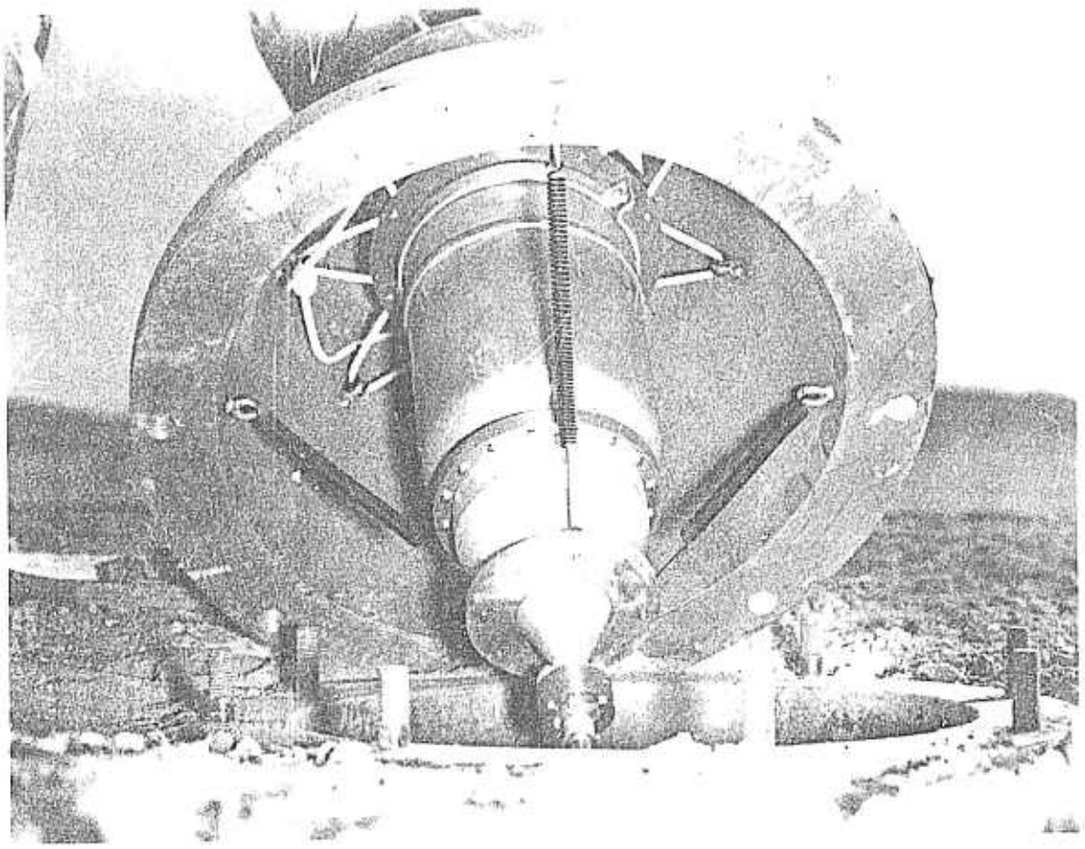

Fig. 2 — View of the detector and the method of mounting it in the aluminum protective dome.

[redacted]

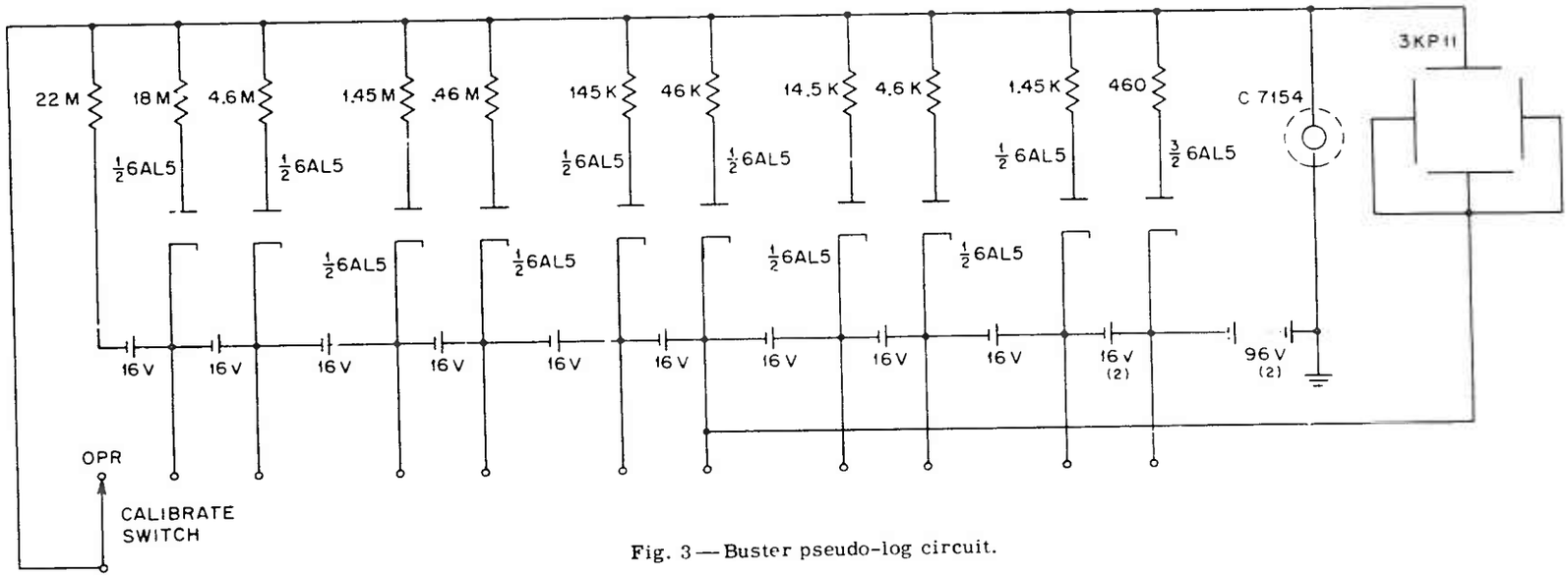

Fig. 3 — Buster pseudo-log circuit.

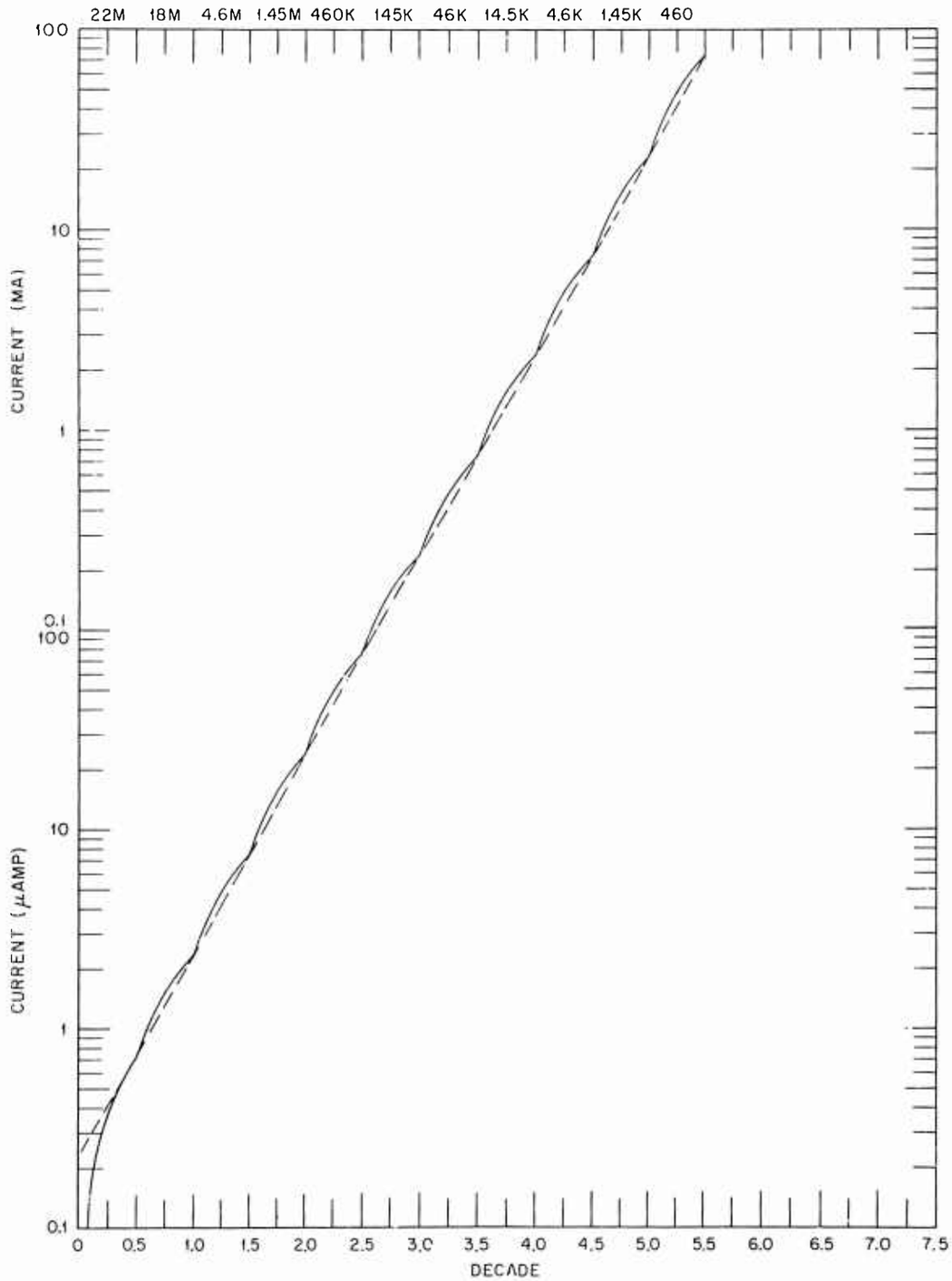

Fig. 4—Pseudo-log circuit characteristic.

[redacted]

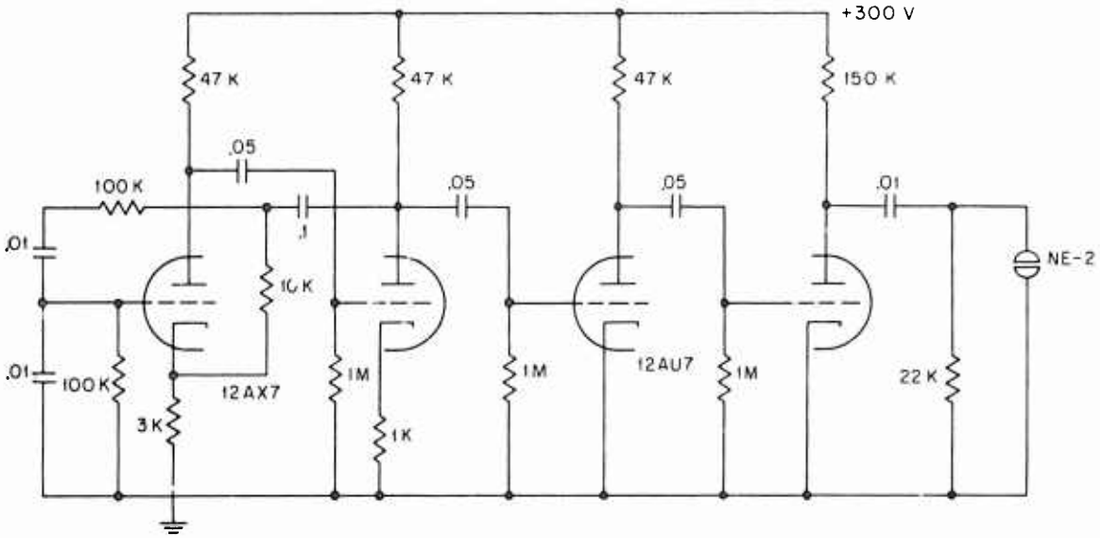

Fig. 5—Timing oscillator. Frequency is 180 cps; batteries are 6-volt U-C Lite and 300-volt Minimax.

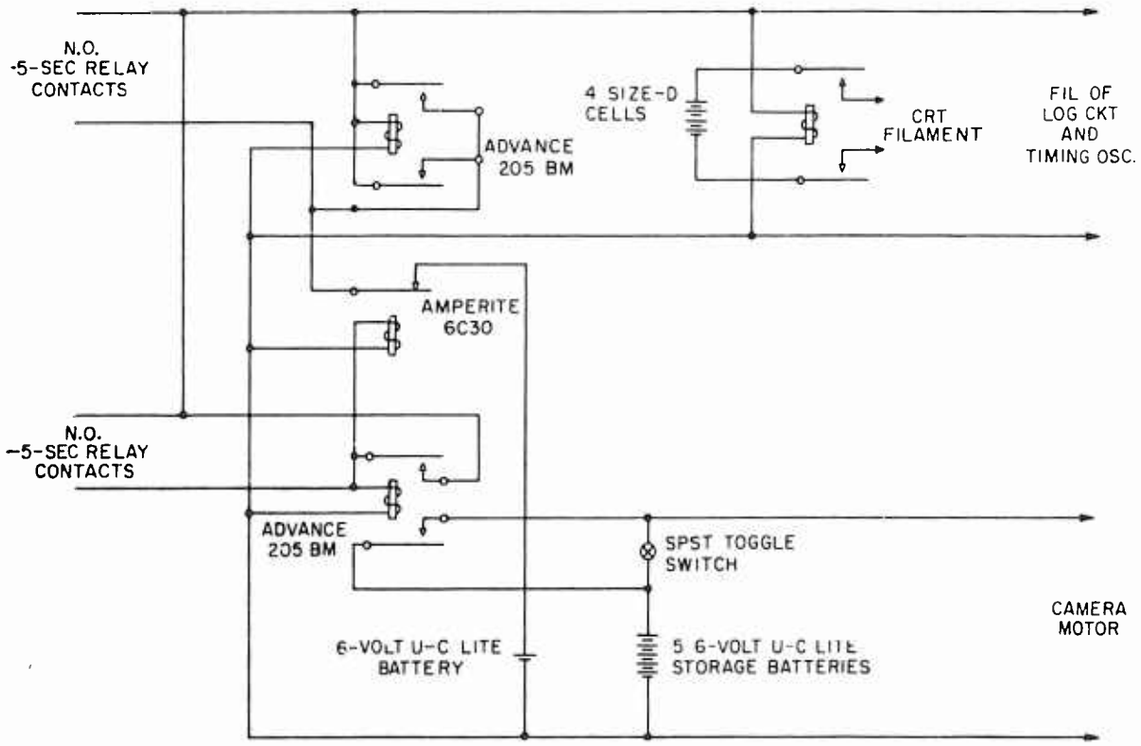

Fig. 6—Control circuit.

[redacted]

can 10 in. in diameter and about 3 ft long, which was then suspended from shock cord in the small culvert so that the camera was about 15 ft below ground level. The enlarged portion of the hole was filled with sandbags as part of the buttoning-up operation. (See Figs. 7, 8, 9, and 10.)

3. CALIBRATION

The detectors were calibrated with the help of LASL Group P-1, who were measuring alpha using the same style detectors. The source used was a 26.6-curie cobalt 60 source, with readings of the current output of the detectors at several distances ranging from 0.5 m to 2.5 m being made by use of a Leeds & Northrup micromicroammeter. A number of readings were taken to get some idea of the departures from inverse r^2 and the degree of scatter, both of which were low.

The log circuits were checked in the laboratory for deviation from the calculated voltage vs current characteristic with the result that the measured values scattered about the calculated curve. On this basis, calibration in the field was carried out by switching in currents corresponding to the diode switching points and recording the corresponding voltage in terms of spot deflection on the initial portion of the shot film. Components of the log circuits were all selected to be within 2 per cent of the desired value. The film was read by use of a Gaertner microcomparator with a reproducibility of about 0.1 per cent in terms of deflection. With these precautions the accuracy of reading the current from the phototube was probably something like 5 per cent.

4. RESULTS

Buster A: No nuclear reaction.
Buster B: −5-min timing signal failed.
Buster C: Good data at both stations.
Buster D: Broken timing wire to far station; camera in near station jammed.
Buster E: Near-camera motor armature opened, causing arcing, which makes data somewhat suspect. Far station OK.
Jangle F: Broken timing wires to far station. Near station OK.

Table 1 summarizes the results obtained. The data are plotted in Figs. 11 through 15. Figures 12 and 14 were obtained by integrating the curves of Figs. 11 and 13, respectively.

For the calculation of source intensities, the following assumptions have been used.

N_2 capture region:

Mean free path in air = 40 g/cm^2

Seven per cent of neutrons captured in N_2 give rise to gammas.

$\sigma_t = 1.86$ barns

Neutrons available for capture $= \nu + \frac{\nu - 1}{e} + \frac{\nu - 1}{e^2} + \ldots = 3.3$ for U^{235}

1.45×10^{23} fissions per kiloton

Fission-fragment region:

Mean free path = 35 g/cm^2

1.45×10^{23} fissions per kiloton

Fragment activity $= 10^{23} e^{-0.106 \ln^2 10.5t}$ for $t < 20$ sec
(P-2 data using radium calibration)

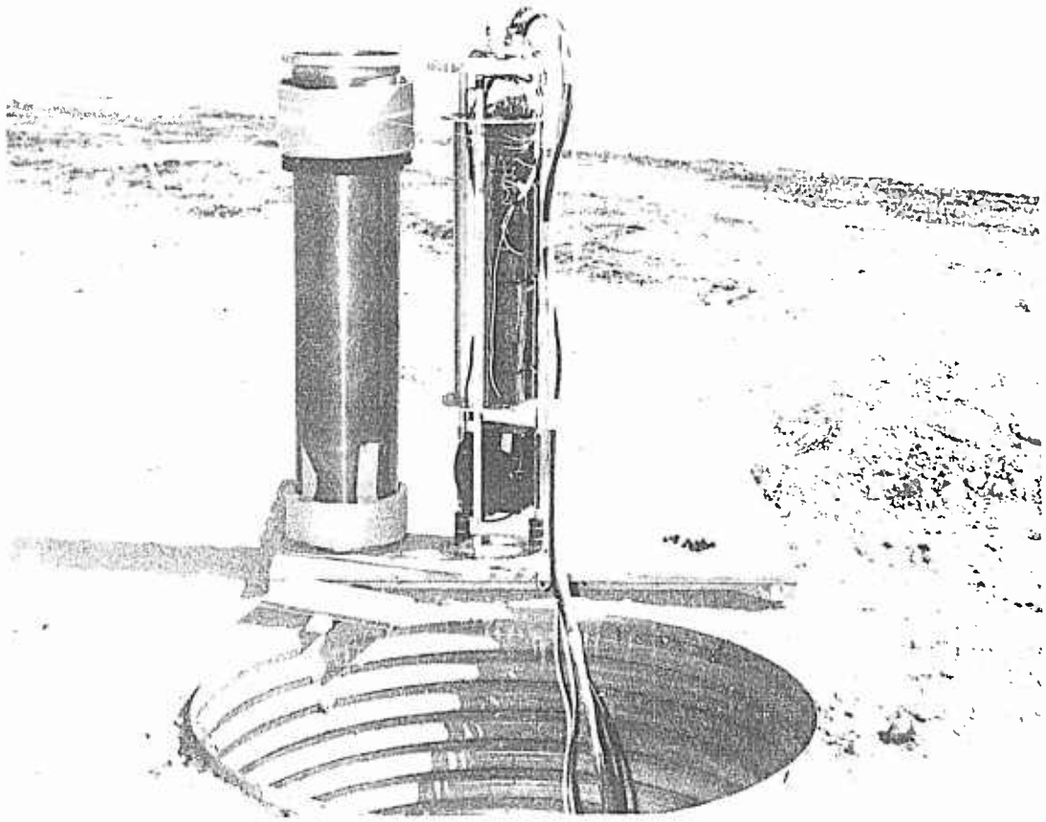

Fig. 7 — Recording unit removed from the can. The 3-in. scope tube is mounted in the aluminum tube at the left with the string of seven 300-volt Minimax batteries together with focus and intensity taps on the right. The camera is at the bottom.

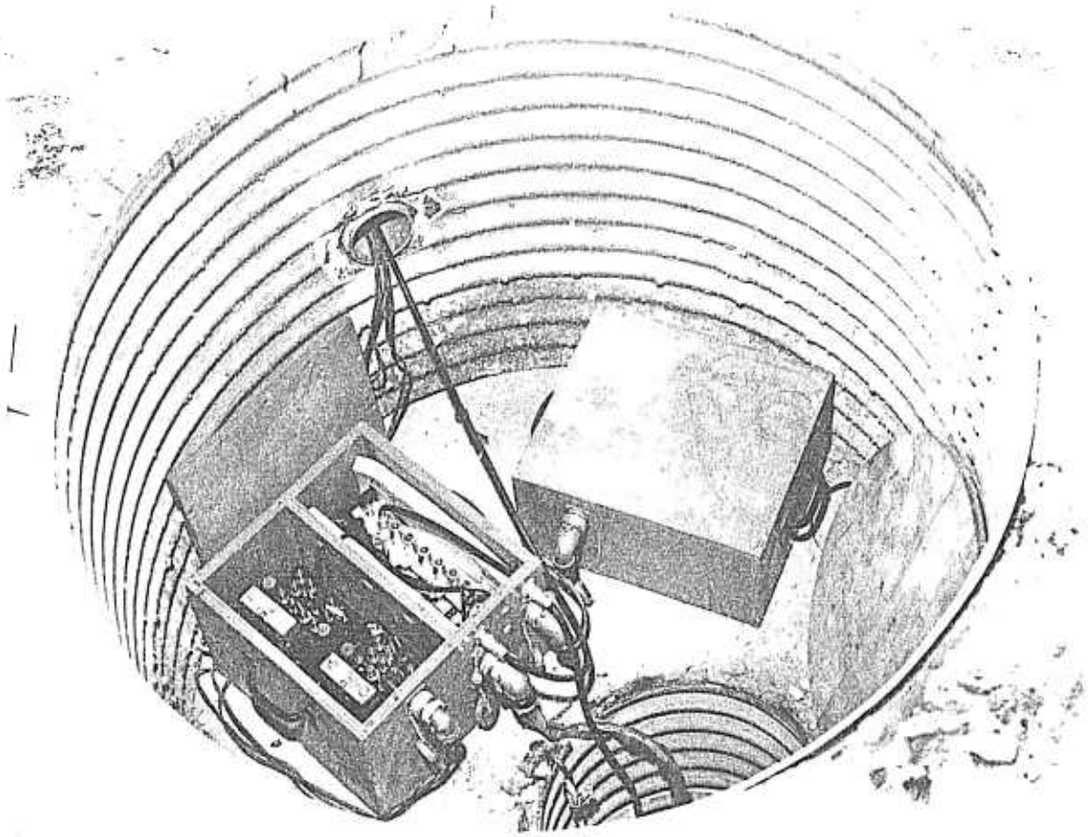

Fig. 8 — Station 961, showing location of the electronics box housing two timing relays, the log circuit and control circuit, and, to the right, the box containing the storage batteries used for filament and camera power. The conduit at the back leads to the detector mount. The culvert into which the recording unit is lowered is at the front of the picture.

[redacted]

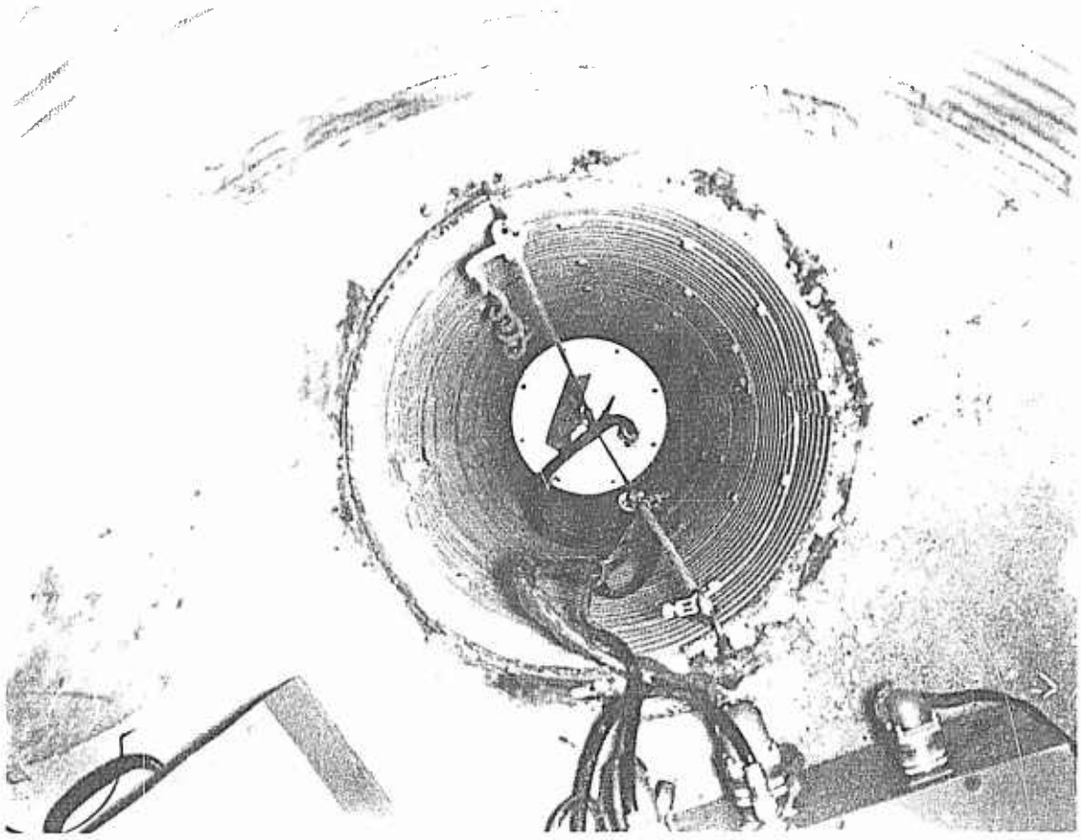

Fig. 9 — The recording unit lowered into the culvert, showing method of suspension.

[redacted]

Fig. 10—Station 961 buttoned up ready for a shot. The large hole has been filled with sandbags, the sandbags covered with a piece of canvas, and the canvas covered with a layer of dirt 2 to 3 in. deep.

[redacted]

Table 1—SUMMARY OF DATA

Test	Range, yd	Radchem yield, kt	N_2 capture						Fission fragments			Total integral, r (including 8% for early γ)	Film badge dose, r
			τ, msec		Source intensity ($\times 10^{23}$ $\gamma/cm^2/sec$)		I_0, r/sec	Integral, r	Source intensity ($\times 10^{23}$ $\gamma/cm^2/sec$)		Integral, r		
			Calculated	Measured	Calculated	Measured			Calculated	Measured			
Buster													
C	610	14.0	73	72	0.68	1.26	76,000	6,000	14.0	10.0	13,000	20,600	20,000
C	1,100	14.0	73	66	0.68	1.4	8,000	530	14.0	9.0	900	1,550	1,350
E	635	31.4		67	1.6	2.4	115,000	8,000	31.4	11.4	10,000	19,500	
E	1,040	31.4		68	1.6	2.2	40,000	2,900	31.4	18.2	3,300	7,000	8,000
Jangie													
F	500	1.2							1.2	0.74	2,000	2,000	2,200

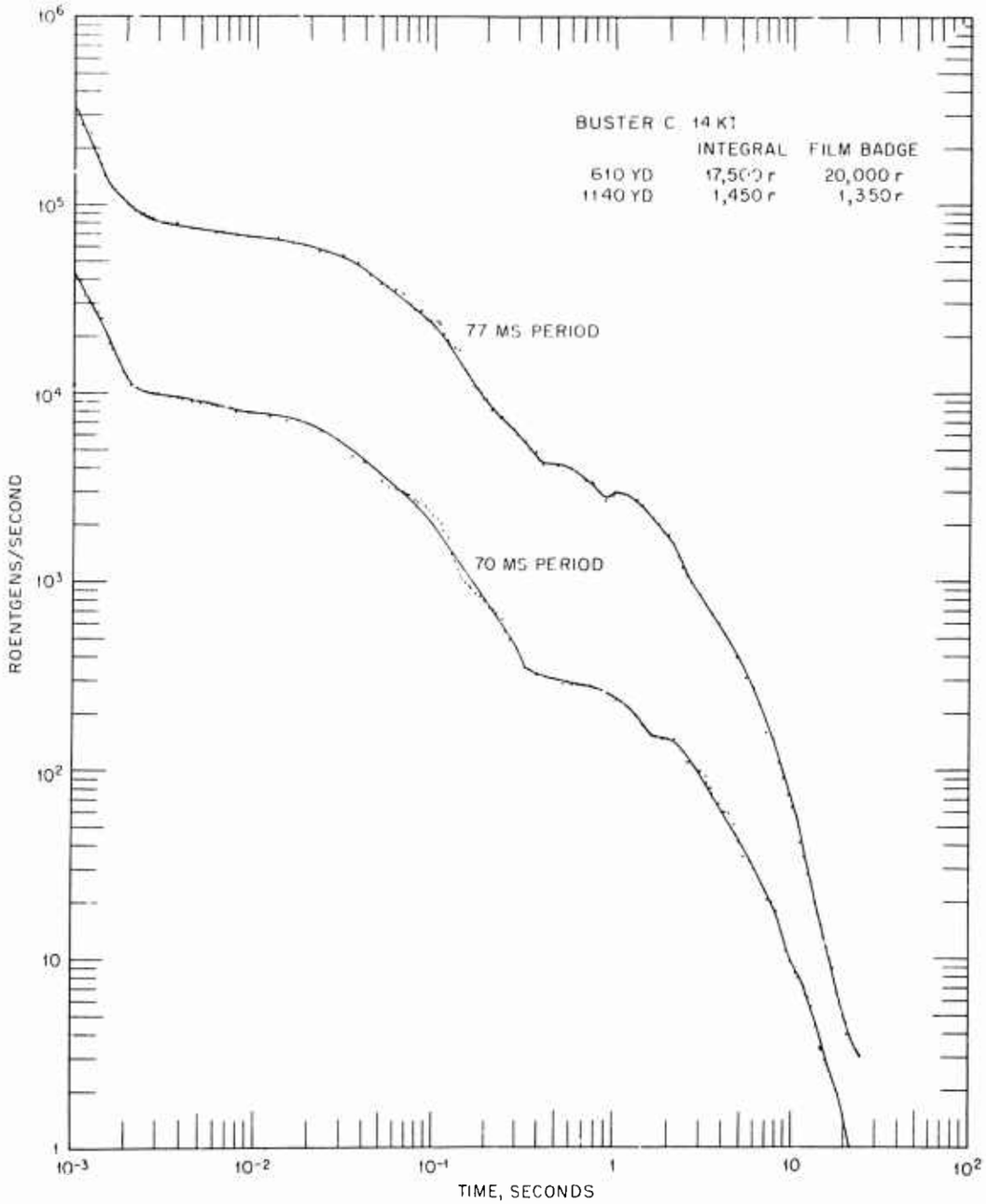

Fig. 11—Gamma intensity vs time, Buster C.

[redacted]

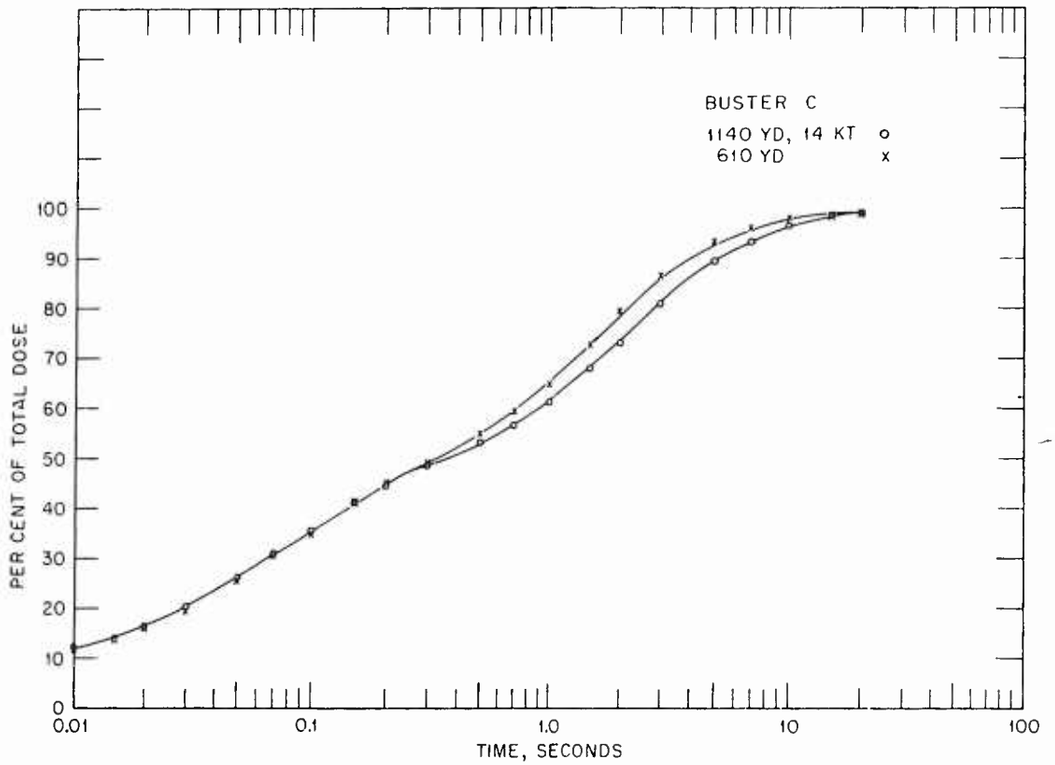

Fig. 12—Integral of curve of Fig. 11.

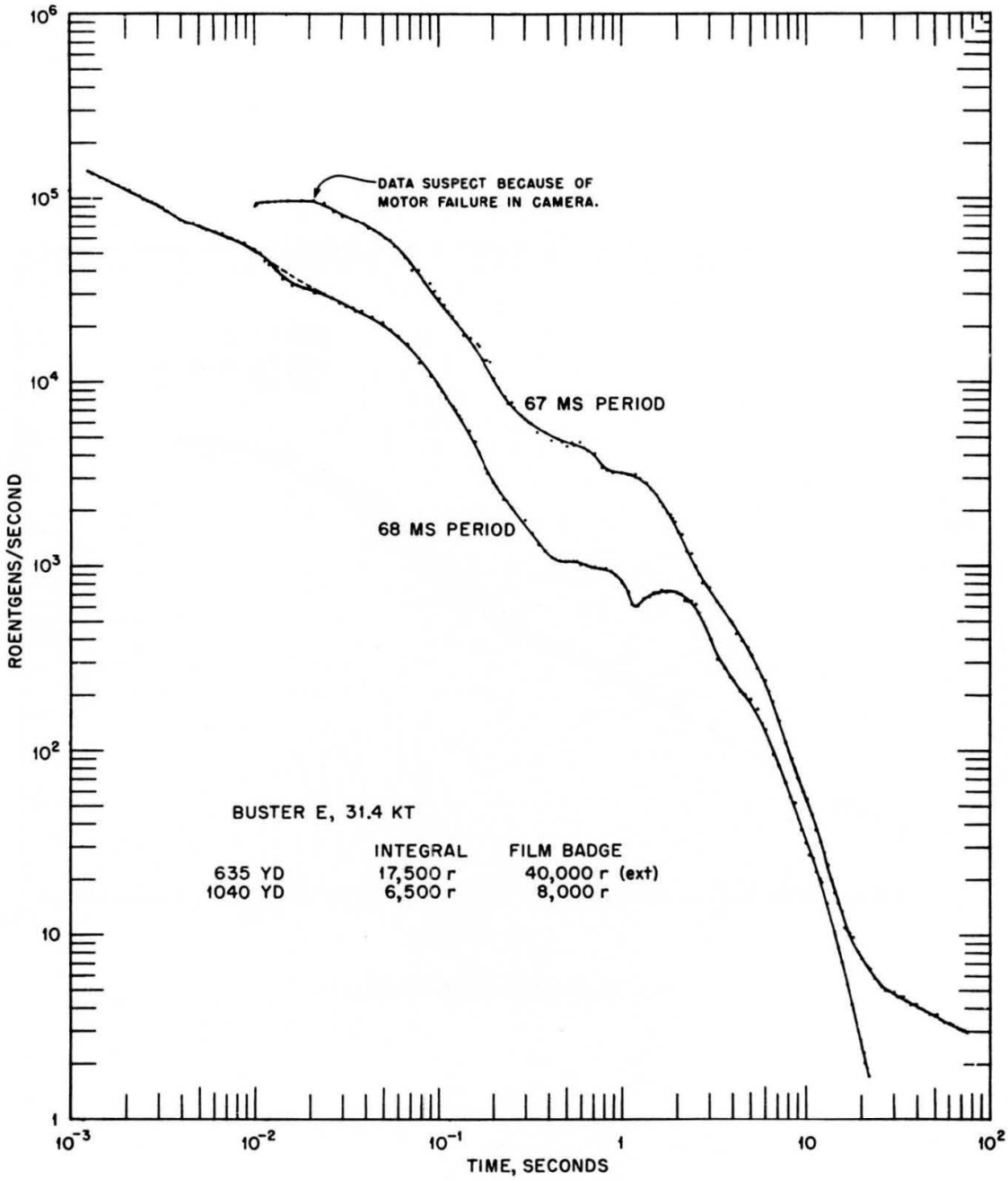

Fig. 13—Gamma intensity vs time, Buster E.

UNCLASSIFIED

[redacted]

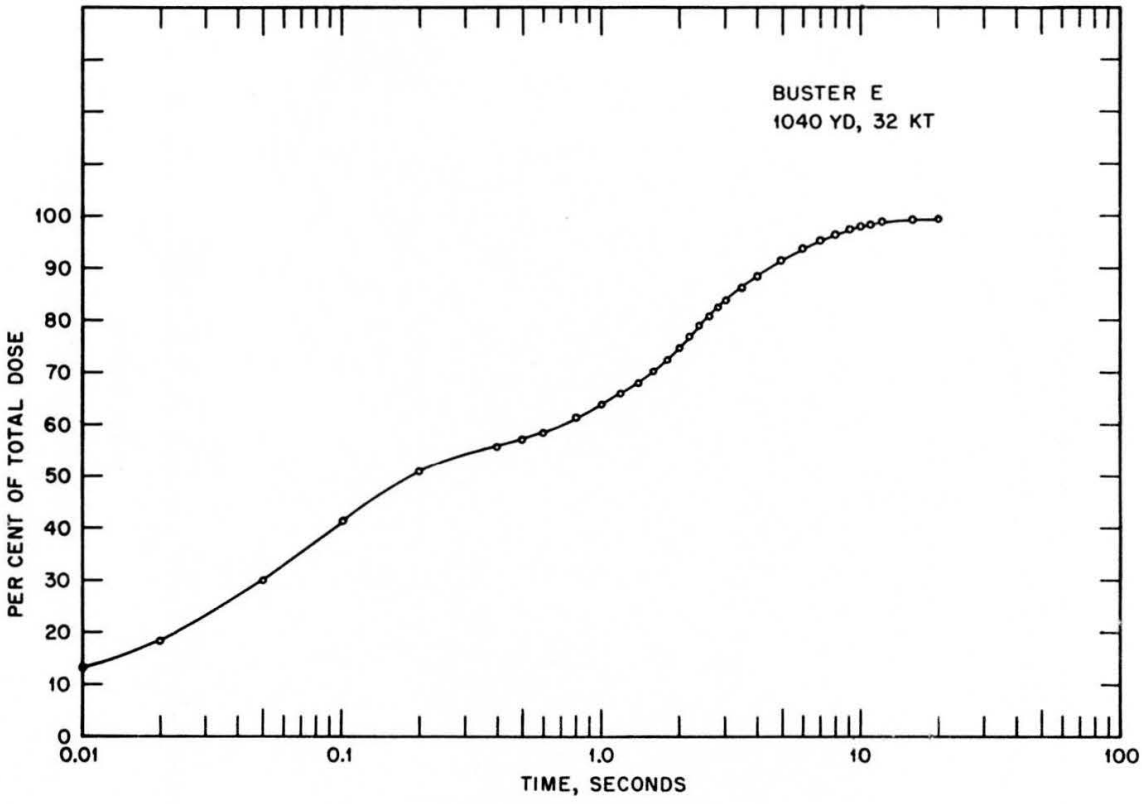

Fig. 14—Integral of curve of Fig. 13.

[redacted]

UNCLASSIFIED

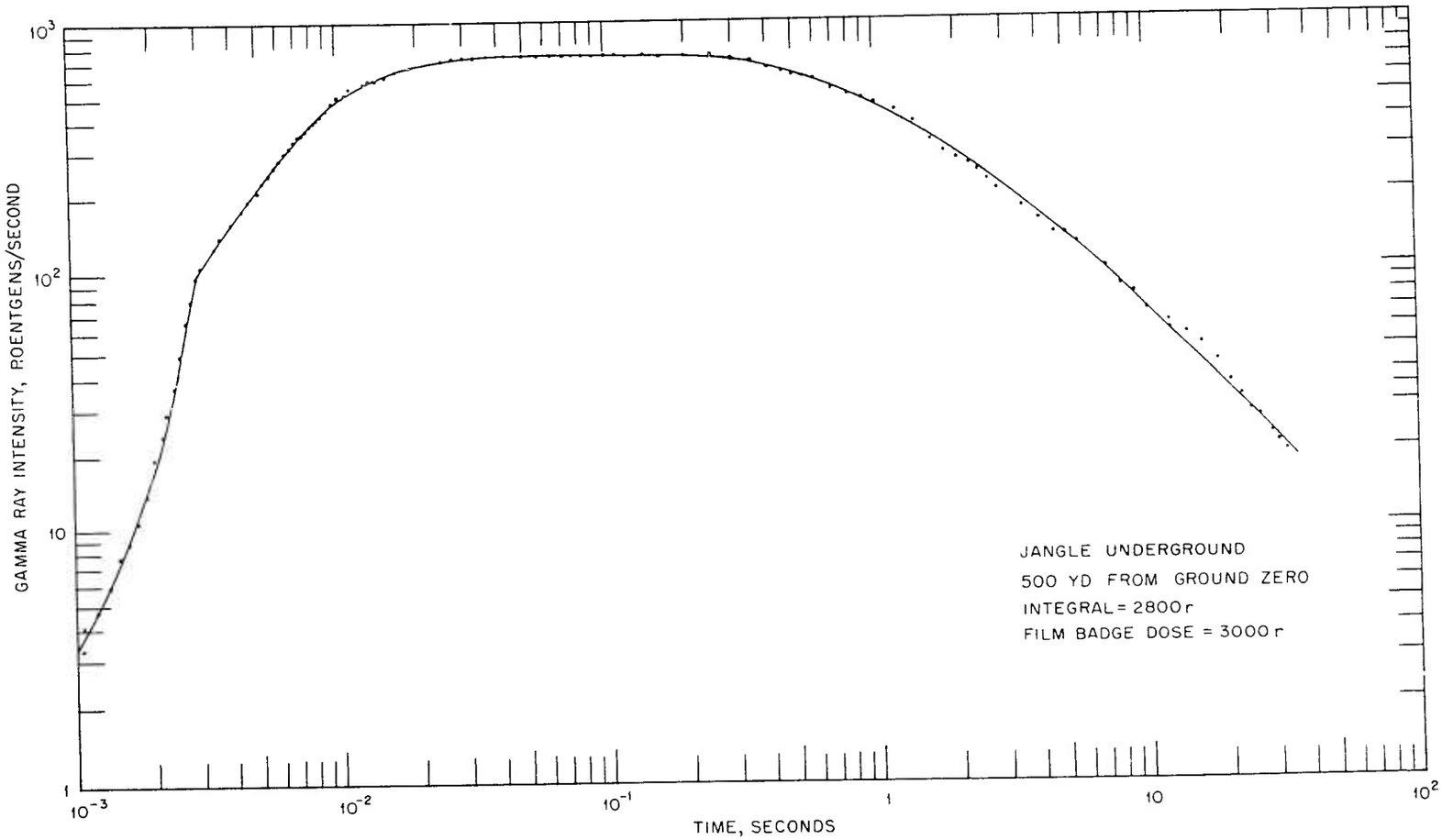

Fig. 15 — Gamma intensity vs time, Jangle F.

For the determination of the total integral, 8 per cent of the integral of these data has been added to include the dose for times less than 1 msec. This number is the result of integrating the data obtained by Hall's group (of the Naval Research Laboratory) on the Greenhouse Easy test.

The measured source intensity for the N_2 capture region is higher than would be expected on the above assumptions owing to an error in mean free paths, detector sensitivity interpretation, insufficient allowance for shock wave, bad guess on number of neutrons present, and/or error in cross section. The agreement is, however, good enough to justify the statement that this is the source of the gamma rays at this time.

For the fission-fragment activity region the measured values are low, perhaps for some of the reasons above and also misinterpretation of the laboratory data.

REFERENCES

1. Pomerance, Reports ORNL-577 and ORNL-366 (quoted in NBS Circular 499).
2. Brolley et al., Report LA-1188 (cyclotron data).
3. B. Watt, private communication (LASL Group P-2 data).

APPENDIX A

PSEUDO-LOG CIRCUIT

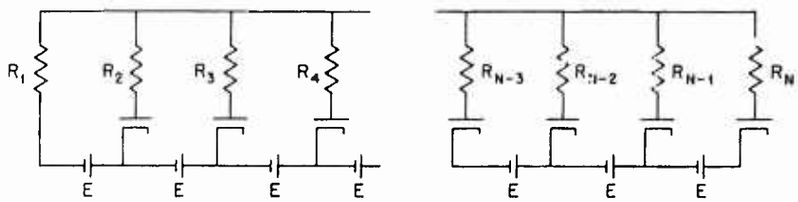

If switching points or cusps are to lie on a straight line on a semilogarithmic plot of current vs output voltage and if ratio of switching currents for two adjacent points is α, then for any resistor R_i ($i > 2$),

$$R_i = \alpha^{N-i} R_N$$

$$R_2 = \alpha^{N-3} \frac{(\alpha - 1)^2}{\alpha - 2} R_N$$

$$R_1 = \alpha^{N-3} (\alpha - 1)^2 R_N$$

α	$\frac{R_1}{R_N}$	$\frac{R_2}{R_N}$	$\frac{R_3}{R_N}$	$\frac{R_4}{R_N}$	...	$\frac{R_{N-1}}{R_N}$
2	2^{N-3}	∞	2^{N-3}	α^{N-4}	...	α
$\sqrt[3]{10}$	$0.618^{(N-1)/3}$	$4.02^{(N-2)/3}$	$10^{(N-3)/3}$	$10^{(N-4)/3}$	...	α
$\sqrt{10}$	$0.467^{(N-1)/2}$	$1.29^{(N-2)/2}$	$10^{(N-3)/2}$	$10^{(N-4)/2}$	...	α
10	$0.81 \times 10^{N-1}$	$1.013 \times 10^{N-2}$	10^{N-3}	10^{N-4}	...	α

Deviation from log response at middle of step:

Actual current:

$$I = \frac{\alpha - 1}{2} \times I_S + I_S = \frac{\alpha + 1}{2} I_S$$

if

$$I_{log} = \sqrt{\alpha}\, I_S$$

$$\frac{I_{actual}}{I_{log}} = \frac{\alpha + 1}{2\sqrt{\alpha}}$$

α	$\frac{I_{actual}}{I_{log}}$
2	1.06
$\sqrt[3]{10}$	1.075
$\sqrt{10}$	1.17
10	1.74

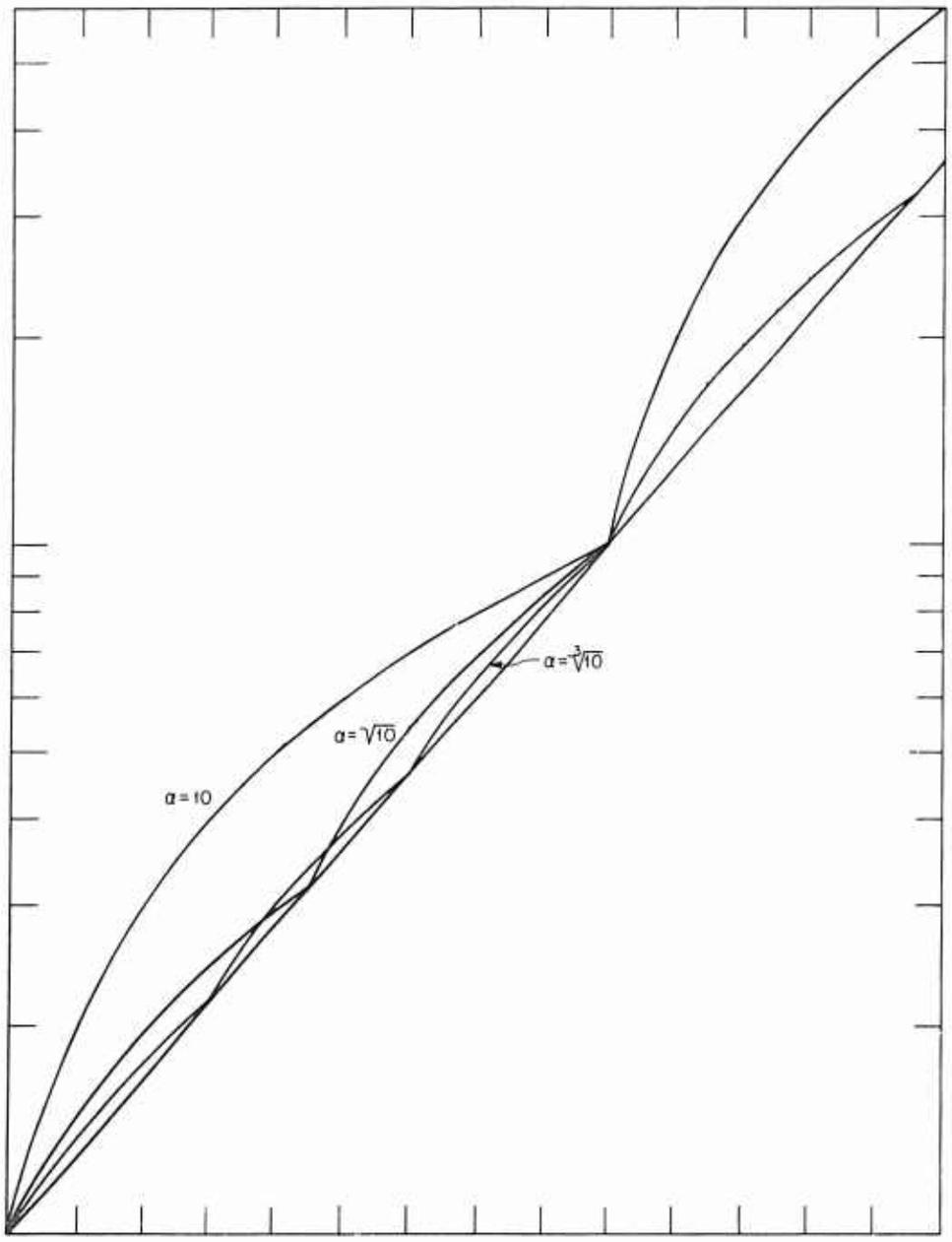

Fig. A.1—Pseudo-log circuit characteristics for various values of alpha.

[redacted]

APPENDIX B

SHIELDING MEASUREMENTS

The results of film-badge measurements at the stations are tabulated below. Station 961 was about 600 yd from ground zero, and Station 962 was about 1100 yd. The results show a shielding factor in dirt of about 6 in. per factor of e for the sandbag shielding and an inverse r^2 shielding for the pipe, assuming a uniform "brightness" at the top of the culvert.

Table B.1 — SHIELDING MEASUREMENTS, BAKER TEST

Measurement	Dose, r	
	Station 961	Station 962
Total dose	5500	400
In conduit (under some 1.5 ft of dirt)	170	16
Top of 18-in. culvert	27	<10
At middle of cable (about 4 ft below top of culvert)	2.6	0.16*
On top of recording can (about 8 ft below top of culvert)	0.8	0.16
At camera	0.11	0.16

* The dose received on the film at this point was probably all due to exposure during recovery, since data from this station were recovered first and the dose received by the recovery party was more than this.

[redacted]

UNCLASSIFIED

Table B.2—SHIELDING MEASUREMENTS, DOG TEST

Measurement	Dose, r
Total dose	$\sim 2 \times 10^4$
In conduit (under some 1.5 ft of dirt)	1200
At electronics box (under some 2.5 ft of sandbags)	>300
At top of 18-in. culvert	140
1.5 ft below top of culvert	58
3 ft below top of culvert	11
5.0 ft below top of culvert	5.2
7 ft below top of culvert	2.0
At relay shelf in recording unit (8.5 ft below top)	1.1
At camera	0.3

[redacted]

DISTRIBUTION

	Copy
ARMY ACTIVITIES	
Chief of Ordnance	1–3
Chief Chemical Officer	4–7
Chief of Engineers	8–10
Quartermaster General	11–15
Chief of Transportation	16–17
Chief Signal Officer	18–20
Surgeon General	21–23
Provost Marshal General	24–26
Chief Army Field Forces	27–30
President, Army Field Forces Board No. 1, Fort Bragg	31
President, Army Field Forces Board No. 2, Fort Knox	32
President, Army Field Forces Board No. 3, Fort Benning	33
President, Army Field Forces Board No. 4, Fort Bliss	34
Commandant, Infantry School, Fort Benning	35–36
Commandant, Armored School, Fort Knox	37–38
President, Artillery School Board, Fort Sill	39–40
Commandant, AA&GM Branch, Artillery School, Fort Bliss	41–42
Commandant, Army War College	43–44
Commandant, Command and General Staff College, Fort Leavenworth	45–46
Commandant, Army General School, Fort Riley	47
Commanding General, First Army, Governor's Island	48–49
Commanding General, Second Army, Fort George G. Meade	50–51
Commanding General, Third Army, Fort McPherson	52–53
Commanding General, Fourth Army, Fort Sam Houston	54–55
Commanding General, Fifth Army, Chicago	56–57
Commanding General, Sixth Army, Presidio of San Francisco	58–59
Commander-in-Chief, European Command	60–61
Commander-in-Chief, Far East	62–63
Commanding General, U. S. Army, Pacific	64–65
Commanding General, U. S. Army, Caribbean	66–67
Commanding General, U. S. Army, Alaska	68–69
Operations Research Office (Johns Hopkins University)	70–72
Commanding Officer, Ballistic Research Laboratories	73–74
Commanding Officer, Engineer Research and Development Laboratory	75–76
Commanding Officer, Signal Corps Engineering Laboratory, Fort Monmouth	77–78
Commanding Officer, Evans Signal Laboratory	79–80
Commanding General, Army Chemical Center, Chemical and Radiological Laboratory	81–82
Assistant Chief of Staff, G-1	83
Assistant Chief of Staff, G-2	84
Assistant Chief of Staff, G-3	85–88
Assistant Chief of Staff, G-4	89–93

[redacted]

UNCLASSIFIED

	Copy
NAVY ACTIVITIES	
Chief of Naval Operations, Op-36	94–95
Chief, Bureau of Ships	96–99
Chief, Bureau of Ordnance	100
Chief, Bureau of Medicine and Surgery	101–102
Chief, Bureau of Aeronautics	103–104
Chief, Bureau of Supplies and Accounts	105–106
Chief, Bureau of Yards and Docks	107–109
Chief of Naval Personnel	110
Commandant of the Marine Corps	111–113
Commander-in-Chief, U. S. Pacific Fleet	114
Commander-in-Chief, U. S. Atlantic Fleet	115
President, U. S. Naval War College, Newport	116
Commandant, Marine Corps Schools, Quantico	117–118
Chief of Naval Research	119–120
Commander, U. S. Naval Ordnance Laboratory	121
Commander, U. S. Naval Ordnance Laboratory (Aliex)	122
Director, U. S. Naval Research Laboratory	123
Commanding Officer and Director, U. S. Naval Electronics Laboratory	124
Commanding Officer, U. S. Naval Radiological Defense Laboratory	125–128
Commanding Officer and Director, David W. Taylor Model Basin	129
Commander, Naval Material Laboratory	130
Officer-in-Charge, U. S. Naval Civil Engineering Research and Evaluation Laboratory	131–132
Commanding Officer, U. S. Naval Medical Research Institute	133
Commander, U. S. Naval Ordnance Test Station, Inyokern	134
AIR FORCE ACTIVITIES	
Assistant for Atomic Energy	135–136
Director of Operations, Operations Analysis Division	137–138
Director of Plans (AFOPD-P1)	139
Director of Requirements	140
Director of Research and Development	141–142
Director of Intelligence (Phys. Vul. Branch, Air Targets Division)	143–144
Director of Installations	145
Assistant for Development Planning	146
Assistant for Materiel Program Control	147
Surgeon General	148
Commanding General, Strategic Air Command, Offutt Air Force Base	149–151
Commanding General, Air Research and Development Command	152–161
Commanding General, Air Materiel Command, Wright-Patterson Air Force Base	162–163
Commanding General, Air Materiel Command, Wright-Patterson Air Force Base, Air Installations Division	164–165
Commanding General, Tactical Air Command, Langley Air Force Base	166–168
Commanding General, Air Defense Command, Ent Air Force Base	169–171
Commanding General, Air Proving Ground, Eglin Air Force Base	172–173
Commanding General, Air Training Command, Scott Air Force Base	174–176
Commanding General, Air University, Maxwell Air Force Base	177–179
Commanding Officer, Special Weapons Center, Kirtland Air Force Base	180–182

UNCLASSIFIED

CANCELLED SECRET UNCLASSIFIED
SECURITY INFORMATION

	Copy
Commanding General, 1009th Special Weapons Squadron	183
Commanding General, Wright Air Development Center, Wright-Patterson Air Force Base	184–187
Commanding General, Air Force Cambridge Research Center	188–189
Commanding General, U. S. Air Forces in Europe	190–191
Commanding General, Far East Air Forces	192–193
Commanding General, Air Force Missile Center, Patrick Air Force Base	194
Commandant, School of Aviation Medicine, Randolph Air Force Base	195
RAND Corporation	196–197
Assistant to the Special Assistant Chief of Staff (Griggs)	198

AFSWP ACTIVITIES

Chief, Armed Forces Special Weapons Project, Washington	199–207
Commanding General, Field Command, Armed Forces Special Weapons Project, Albuquerque	208–210
Commanding Officer, Test Command, Armed Forces Special Weapons Project, Albuquerque	211–213

ATOMIC ENERGY COMMISSION

Atomic Energy Commission, Washington	214–216
Los Alamos Scientific Laboratory, Report Library	217–236
Sandia Corporation	237–256
Technical Information Service, Oak Ridge (surplus)	257–294
University of California Radiation Laboratory (York)	295
Weapon Test Reports Group, TIS	296

DEPARTMENT OF DEFENSE

Chairman, Research and Development Board	297
Director, Weapons System Evaluations Group, Office of the Secretary of Defense	298
Executive Director, Committee on Atomic Energy, Research and Development Board (Beckler)	299
Executive Director, Committee on Medical Sciences, Research and Development Board	300

UNCLASSIFIED

SECRET
SECURITY INFORMATION

AEC, Oak Ridge, Tenn., A31923